Molecule without Electrons: Binding Bare Nuclei with Strong Laser Fields

Olga Smirnova
Department of Physics, Moscow State University, Vorobievy Gory, Moscow, 119 992 Russia

Michael Spanner
Department of Physics, University of Waterloo, Waterloo, Ontario, Canada N2L 3G1
and NRC Canada, 100 Sussex Drive, Ottawa, Ontario, Canada K1A 0R6

Misha Ivanov
NRC Canada, 100 Sussex Drive, Ottawa, Ontario, Canada K1A 0R6
(Received 20 September 2002; published 16 June 2003)

We show how a carefully chosen combination of strong linearly and circularly polarized laser fields can bind two same-sign charges, not only suppressing their Coulomb repulsion in all three spatial dimensions, but also creating an effective attraction. As an example, we show how a molecule HD^{2+} stripped of both electrons can be kept bound by the laser fields.

DOI: 10.1103/PhysRevLett.90.243001 PACS numbers: 33.80.Rv, 33.80.Wz, 42.50.Hz

As known to any juggler holding a stick on the tip of a finger, rapid oscillations can turn a fully repulsive potential into an effective time-averaged attraction [Fig. 1(a)]. This physics appears in the Kapitza pendulum [1] and in Paul's trap [2].

We show numerically and analytically that a similar principle can be applied to the repulsive Coulomb potential in all three dimensions (3D), with carefully crafted oscillating electric fields working as a juggler to create an effective attraction. However, the physics behind the attraction is fundamentally different from the simple 1D case shown in Fig. 1(a) (see also [3]). For same-sign charges, a purely static effective potential which comes from averaging the charge motion over the oscillation period as in Fig. 1(a) cannot create attraction in all three dimensions (the Earnshaw theorem [4]). Here, the crucial role is played by the *dynamical* corrections to the period-averaged motion, getting around the Earnshaw theorem and making the effect similar to stable levitation of magnets in levitrons [5]. Levitrons get around the Earnshaw theorem in a similar way—by spinning the object.

To illustrate the effect, we show how a combination of linearly and circularly polarized laser fields can bind H^+ and D^+ into a stable "molecule" HD^{2+}. The different charge to mass ratio for the nuclei is critical: otherwise, their relative motion is unaffected by the laser fields.

The idea of using oscillations in strong laser fields to stabilize a system of charged particles has been studied extensively. For example, a laser field can be used to stabilize H^{2-} [6]. However, all previous cases have dealt with charges of opposite signs, e.g., using the laser field to distribute the attraction of a single proton between three electrons in H^{2-}. We deal with same-sign charges, and therein lies the fundamental physical difference. In all previous cases the cycle-averaged potential provides stabilization and the dynamical corrections are the source of the decay of a metastable state. Here, the cycle-average potential *is not binding*; it is the dynamical corrections which are responsible for stabilization.

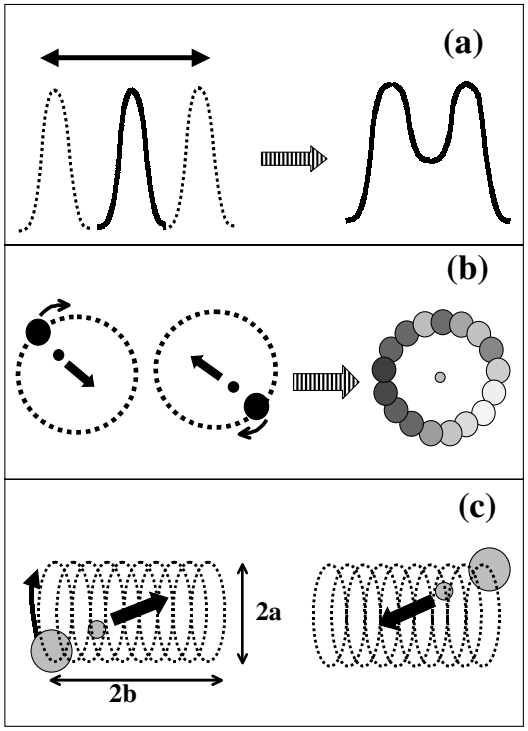

FIG. 1. Binding two same-sign charges with oscillating electric fields. (a) The 1D case requires a linearly polarized field; (b) the 2D case requires a circularly polarized field; (c) the 3D case requires circularly and linearly polarized fields, with *a* and *b* defining the laser-driven trajectory. Note that cycle-averaged potential alone cannot bind in 3D.

In the center-of-mass reference frame the Hamiltonian of the relative motion of the two charges is

$$H = \frac{p^2}{2\mu} - \frac{q}{c}\frac{\mathbf{pA}}{\mu} + \frac{Q_1Q_2}{R} + \frac{A^2}{2c^2}\left(\frac{Q_1^2}{M_1} + \frac{Q_2^2}{M_2}\right), \quad (1)$$

where $\mathbf{A}$ is the vector potential of the laser field, the effective charge is $q = \mu(Q_1/M_1 - Q_2/M_2)$, and the reduced mass is $\mu = M_1M_2/(M_1 + M_2)$.

It is instructive to start with the 2D case to clarify the physics and underline the special aspects of the 3D case. In 2D the attraction requires a circularly polarized field $\mathbf{A}(t) = (cE/\omega)\{-\sin\omega t, \cos\omega t, 0\}$, i.e., two orthogonal linearly polarized fields. Without the Coulomb potential, the particle with the charge $q = \mu(Q_1/M_1 - Q_2/M_2)$ and mass $\mu = M_2M_1/(M_1 + M_2)$ would have run on a circle of the radius $a = qE/\mu\omega^2$. In the reference frame of this particle, it is the repulsive Coulomb center that runs on the circle, Fig. 1(b). Over one revolution, kicks from the Coulomb potential occur in all radial directions, exactly compensating each other in the center. Displacement from the center leads to an effective restoring force—the Coulomb force is stronger on the side of the circle that moved closer to the center of mass. Over the laser cycle, in this reference frame the Coulomb center forms a 2D cage which can keep the particle inside.

Mathematically, the above picture is described by switching to the so-called Kramers-Henneberger (KH) reference frame x', y', z' [7] which for the vector potential $\mathbf{A}(t) = A\{-\sin\omega t, \cos\omega t, 0\}$ is defined by the variable substitution $x = x' + a\cos\omega t$, $y = y' + a\sin\omega t$, $z = z'$. It describes motion of the reduced system (charge q, mass μ) in the laser field only. In the KH frame, interactions with the Coulomb potential and the laser field are replaced by the single time-dependent potential

$$U(\mathbf{R}', t) = \frac{Q_1Q_2}{\sqrt{(x' + a\cos\omega t)^2 + (y' + a\sin\omega t)^2 + z'^2}}. \quad (2)$$

In the 2D case z' is fixed. For sufficiently large ω the dynamics is dominated by the cycle-averaged potential

$$U^{\mathrm{KH}}(\mathbf{R}') = \int_0^{2\pi} \frac{Q_1Q_2 d\phi/2\pi}{\sqrt{(x' + a\cos\phi)^2 + (y' + a\sin\phi)^2 + z'^2}}, \quad (3)$$

which develops a well as seen in Fig. 2(a). The averaging procedure is valid if (i) the laser field dominates the Coulomb repulsion, and (ii) the change ΔR in the relative distance between the particles during the oscillation period is small compared to the initial distance R_0 [8]. Trapping requires $R_0 < a = qE/\mu\omega^2$ to ensure that the particle starts inside the cage.

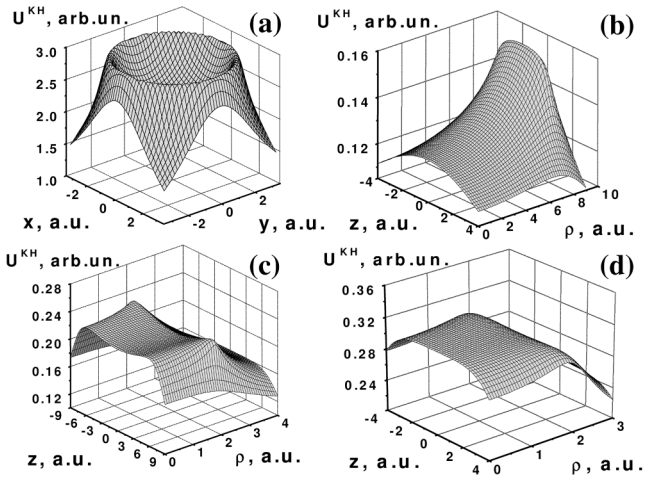

FIG. 2. Average potential U^{KH}: (a) binding in 2D ($a = 3$ a.u.); (b) "weak" linear field $b/a < \kappa_0$ ($b = 2$ a.u., $a = 8$ a.u.)—the repulsion is along the z axis; (c) "strong" linear field $b/a > \kappa_0$ ($b = 8$ a.u., $a = 2$ a.u.)—the repulsion is in the radial direction; (d) for $b/a = \kappa_0$ ($b \approx 4.36$ a.u., $a = 2$ a.u.) the potential is flat inside the cylinder.

Trapping in the 3D case requires a 3D cage, which could be built by two fields: circularly polarized (E_1, ω_1) in the x, y plane and linearly polarized (E_2, ω_2) along z [Fig. 1(c)]. The purely oscillatory motion in these fields $\mathbf{r}_{\mathrm{osc}}(t)$ defines the transformation to the KH frame $\mathbf{R}'$:

$$\mathbf{R} = \mathbf{R}' + \mathbf{r}_{\mathrm{osc}}(t);$$
$$\mathbf{r}_{\mathrm{osc}}(t) = \{a\cos\omega_1 t, a\sin\omega_1 t, b\cos\omega_2 t\}, \quad (4)$$
$$a = qE_1/\mu\omega_1^2; \qquad b = qE_2/\mu\omega_2^2.$$

In the KH frame, the Coulomb center moves on the cylinder with the diameter $2a$ and the height $2b$, Fig. 1(c). The surface of the cylinder is densely covered if one uses incommensurate frequencies ω_1 and ω_2. In the KH frame the exact dynamics is described by the potential

$$U(\mathbf{R}', t) = \frac{Q_1Q_2}{|\mathbf{R}' + \mathbf{r}_{\mathrm{osc}}(t)|}. \quad (5)$$

The cycle-averaged potential is

$$U^{\mathrm{KH}}(\mathbf{R}') = \frac{Q_1Q_2}{(2\pi)^2}\int_0^{2\pi} d\phi_2 \int_0^{2\pi} d\phi_1 \frac{1}{\sqrt{(x' + a\cos\phi_1)^2 + (y' + a\sin\phi_1)^2 + (z' + b\cos\phi_2)^2}}. \quad (6)$$

Contrary to the 1D and 2D cases, in the 3D case the potential cannot be attractive in all three dimensions. Indeed, Eq. (6) describes the electrostatic potential created by the (inhomogeneous) charge distribution on a cylinder with the diameter $2a$ and height $2b$. According to the Earnshaw theorem, nowhere inside the cylinder is this potential attractive in all 3D. Inside the cylinder the potential Eq. (6) satisfies the Poisson equation with a zero right-hand side, allowing only for the saddle-type

geometry at the origin ($x' = y' = z' = 0$). One can check that at the origin $U^{\rm KH}_{x'x'} = U^{\rm KH}_{y'y'} = -(1/2)U^{\rm KH}_{z'z'}$, while all first and mixed second derivatives are equal to zero.

Two things have to be mentioned: (i) it is still possible to have all second derivatives equal to zero, making the potential flat near the origin, and (ii) the averaged potential Eq. (6) is only the first term in the Fourier expansion of the exact time-dependent potential Eq. (5). When it is flat, the higher-order terms become crucial.

The values of a and b (the radius and half-height of the cylinder) for which the KH potential becomes flat near the origin are found by solving $U^{\rm KH}_{x'x'} = 0$. The solution depends only on the ratio b/a, and is equal to $b/a = \kappa_0 = 2.1797\ldots$. The KH potential is shown in Figs. 2(b)–2(d). If $b/a < \kappa_0$ [circular field dominates, Fig. 2(b)], binding occurs in the xy plane and the charges fly apart along z. For $b/a > \kappa_0$ [linear field dominates, Fig. 2(c)] binding occurs in the z direction and the charges fly apart in the xy plane. For $b/a = \kappa_0$ [Fig. 2(d)] the potential is essentially flat inside the cylinder and on average the Coulomb repulsion is eliminated.

Thus, when the strengths of the circular and linear fields are matched, $b/a = \kappa_0$, the dynamics is dominated by the oscillating terms in the Fourier expansion of Eq. (5):

$$U(\mathbf{R}', t) = U^{\rm KH}(\mathbf{R}') + \sum_{n\neq 0}\sum_{k>0} U_{nk}(\mathbf{R}')e^{-in\omega_1 t}\cos k\omega_2 t, \tag{7}$$

where the $\sin k\omega_2 t$ terms are absent due to parity. For high $\omega_{1,2}$ terms $U_{nk}\exp(-in\omega_1 t)\cos k\omega_2 t$ could form an effective ponderomotive-type potential

$$V_{\rm eff} = \sum_n\sum_k V_{nk},$$
$$V_{nk} \propto \frac{(\nabla U_{nk})^2}{\mu}\left(\frac{1}{(n\omega_1 + k\omega_2)^2} + \frac{1}{(n\omega_1 - k\omega_2)^2}\right). \tag{8}$$

$V_{\rm eff}$ can provide binding since U_{nk} are inhomogeneous. Studying the second order derivatives of V_{nk} Eq. (8) at the origin we have checked analytically that $V_{\rm eff}$ is binding.

However, $V_{\rm eff}$ does not always give a complete quantitative description of the dynamics. The binding can have a truly dynamic nature, as in Fig. 3. Strong deviations from the regime described by $V_{\rm eff}$ occur when $\omega_{1,2}$ or $n\omega_1 - k\omega_2$ are not high enough. In the example below (Fig. 3) the latter is the case: $\Omega \equiv 2\omega_1 - \omega_2 \approx 0.1\omega_1$. For commensurate frequencies, e.g., $\omega_2 = 2\omega_1$, terms with $n = 2k$ in Eq. (7) become time independent. Their structure is critical and, according to our simulations, accelerates the decay of the metastable state: for commensurate frequencies the cage in Fig. 1(c) contains holes.

Thus, changing the laser intensities while keeping $b/a = \kappa_0$ constant, we should see three qualitatively different regimes of the dynamics. For relatively weak fields, $a \ll 1$, the flat portion of the potential $U^{\rm KH}$ is too narrow, yielding standard Coulomb repulsion. In the intermediate case $a \sim 1$ we should see binding due to the higher-order terms in Eq. (7). For very high intensities, $a \gg 1$, U_{nk} become too small, the effective potential is flat, and the charges drift apart with constant velocity.

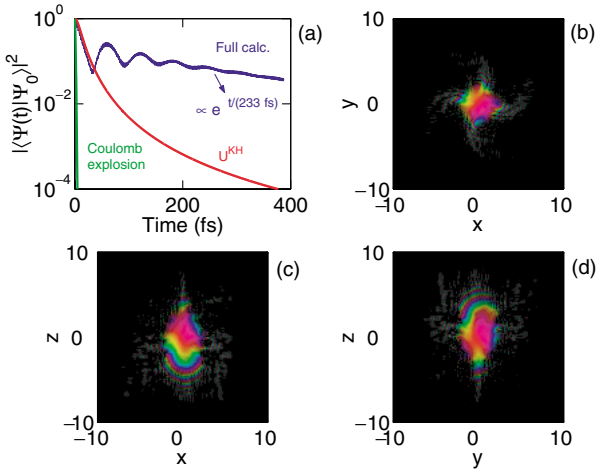

FIG. 3 (color online). Laser-induced bonding in HD^{2+} for $a = 2.5$ and $b \approx 5.45 \approx \kappa_0 a$, $\lambda_1 = 760$ nm (circular, xy plane) and $\lambda_2 = 400$ nm (linear, z axis) (see text). (a) shows $\chi(t) = |\langle\Psi_0|\Psi(t)\rangle|^2$ for the full calculation, $U^{\rm KH}$ only, and the field-free Coulomb explosion. (b)–(d) show sections of the metastable state at $t = 400$ fs. Colors code the wave packet phase (0: red, $2\pi/3$: green, $4\pi/3$: blue); visibility (brightness) codes the wave packet amplitude using a log scale.

In Fig. 3 we show the results of fully quantum numerical simulations of the time-dependent Schrödinger equation for the laser-created molecule HD^{2+}. The calculation is done in the KH frame using a split-operator method in Cartesian coordinates, in all 3D. Absorbing boundaries are introduced using the prescription of [9]. We used 128 grid points per dimension, with a range $-10 \leq x, y, z \leq 10$ and time step 0.047 fs. Convergence was checked by varying the grid size and the time step. Accuracy was further monitored by performing additional 2D calculations for the same grid, with one of the coordinates fixed and the remaining two allowed to evolve. These latter calculations were then also performed with much improved temporal and spatial accuracy to check that the 3D grid gave adequately converged results. For all calculations in Fig. 3 we keep $b/a = 2.1797$. Since the nuclei are rather heavy, the intensities required to reach the regime of interest are high: $a = 1$ requires $I_1 = 5 \times 10^{18}$ W/cm^2 for $\lambda_1 = 800$ nm (within the reach of modern systems [10]). The Lorentz force is unimportant until $I > 10^{22}$ W/cm^2.

To find the metastable state and analyze its long-term dynamics we propagate $\Psi_0 \propto e^{-(x'^2+y'^2)/\sigma_1^2}e^{-z'^2/\sigma_2^2}$ ($\sigma_1 = 0.6$ a.u. and $\sigma_2 = 1.2$ a.u. reflect the cage symmetry) in the presence of the laser fields until 400 fs (Fig. 3). The long-term behavior of $\Psi(t)$ is independent of Ψ_0: the unbound component of Ψ_0 quickly dissociates leaving

only the metastable component. Figure 3 shows the squared autocorrelation function $\chi(t) = |\langle\Psi_0|\Psi(t)\rangle|^2$ for $\lambda_1 = 760$ nm, $\lambda_2 = 400$ nm, and $a = 2.5$. The dynamics of $\chi(t)$ reflects dissociation of HD^{2+}. (We have checked that the norm inside the absorbing boundary decays similarly.) Figure 3(a) also shows $\chi(t)$ for the cycle-averaged potential U^{KH} only and for the field-free Coulomb explosion.

The creation of the metastable molecule is evident in Fig. 3. The long-time decay is exponential, with a characteristic time constant of 233 fs. Fast initial decay, which is similar for U^{KH} and for the full calculation, is followed by dynamic stabilization which is independent of initial Ψ_0. Slow oscillations in $\chi(t)$ have frequency $\Omega = 2\omega_1 - \omega_2$. These oscillations stress the dynamical nature of the metastable state: they cannot be described by V_{eff} and are due to U_{21}, $U_{-2,1}$ in Eq. (7). Classical trajectories remain inside the cage [Fig. 1(c)] for much longer times. Since there is no stationary potential barrier they have to overcome, the nonclassical decay mechanism is dynamic tunneling through the cage boundaries.

Figures 3(b)–3(d) show three sections of the metastable state at $t = 400$ fs. Swirling jets in the xy section demonstrate the decay of the state; the logarithmic scale is used to enhance the jets' visibility. The rainbow profile across the wave packet, which oscillates with laser frequencies $\omega_{1,2}$, shows the spatial phase of the wave function $\Psi(\mathbf{R}')$. Jets slowly rotate with the frequency Ω around the z axis. The same rotation interchanges the xz and yz sections, stressing the dynamical nature of the metastable state.

Creation of the metastable state of HD^{2+} requires the careful balance of laser fields. As in usual scattering, this half-scattering will map the effective potential into energy-angular distribution of the fragments, with the metastable state leaving a resonance signature in the fragment spectrum. Transition to the new regime of Coulomb explosion can also be seen by using only linearly or only circularly polarized fields. A sufficiently strong field linearly polarized along the z axis will provide confinement in z, squeezing the otherwise symmetric Coulomb explosion into a pancake in the xy plane. Alternatively, if only the circular field is present, fragmentation will be squeezed along the propagation direction of the field. Numerical simulations [8] show that strong confinement of the HD explosion to the xy plane requires a linearly polarized field with $I \sim 10^{21}$ W/cm^2 at $\lambda = 800$ nm. To avoid substantial nuclear motion before reaching the required intensities, one needs a fast turn-on of the pulse: for a Gaussian turn-on it is 5 fs half width at half maximum [11]. Under these conditions, enhanced ionization [12], which occurs at bond distances $R_c \sim 4$ Å, is completely suppressed.

Engineering sharp (~ 5 fs) pulse fronts could open an opportunity to keep charged nuclei together—despite their Coulomb repulsion—until the laser field reaches extreme intensities $I > 10^{22}$ W/cm^2. Similar to the conventional electron-ion recollision [13], a recollision between a heavy nucleus and a light proton could then be timed with sub-laser-cycle precision. For a proton, the recollision energy reaches 1 MeV at $I = 10^{22}$ W/cm^2 for 800 nm light, provoking an intriguing thought of stimulating high-energy nuclear collisions with sub-fs accuracy. The effect described here applies to other particles with different charge-to-mass ratio. How it manifests itself in many-particle systems, including explosions of HD clusters at extreme intensities [14], is an open question.

We thank A. Popov, M. Fedorov, H. Batelaan, P. Corkum, G. Yudin, M. Stockman, and V. Gridchin for valuable discussions. This work was supported by RFBR Grants No. 00-02-16046 and No. 02-02-06248, INTAS Grant No. 99-1495, and NSERC Canada through the IOF grant for the Russian-Canadian Photonics network.

[1] See, e.g., L. D. Landau and E. M. Lifshitz, *Classical Mechanics* (Pergamon Press, New York, 1960).
[2] See, e.g., P. K. Ghosh, *Ion Traps* (Clarendon Press, Oxford, 1995).
[3] R. V. Karapetyan, Laser Phys. **10**, 160 (2000).
[4] S. Earnshaw, Trans. Cambridge Philos. Soc. **7**, 97–112 (1842); see also M. V. Berry and A. K. Geim, Eur. J. Phys. **18**, 307 (1997).
[5] M. V. Berry, Proc. R. Soc. London, Ser. A **452**, 1207 (1996); M. D. Simon *et al.*, Am. J. Phys. **65**, 286 (1997); R. Harrigan, U.S. Patent No. 4,382,245 (1983); see also A. K. Geim *et al.*, Nature (London) **400**, 323 (1999).
[6] E. van Duijn, M. Gavrila, and H. G. Muller, Phys. Rev. Lett. **77**, 3759 (1996).
[7] H. A. Kramers, Les Particles Elementaires, Report to the Eighth Solvay Conference, Brusseles: Editions Stoops (1950); W. C. Henneberger, Phys. Rev. Lett. **21**, 838 (1968).
[8] V. V. Gridchin, A. M. Popov, and O. V. Smirnova, Laser Phys. **12**, 182 (2002).
[9] D. E. Manolopoulos, J. Chem. Phys. **117**, 9552 (2002).
[10] See, e.g., T. Brabec and F. Krausz, Rev. Mod. Phys. **72**, 545 (2000).
[11] O. Smirnova, M. Spanner, and M. Ivanov (to be published).
[12] See, e.g., T. Seideman, M. Ivanov, and P. Corkum, Phys. Rev. Lett. **75**, 2819 (1995); T. Zuo and A. Bandrauk, Phys. Rev. A **52**, R2511 (1995).
[13] P. B. Corkum, Phys. Rev. Lett. **71**, 1994 (1995).
[14] See, e.g., T. Ditmire *et al.*, Nature (London) **398**, 489 (1999).